



universität
wien



Yale University
School of Medicine

MARSHALL PLAN SCHOLARSHIP FINAL REPORT

Investigation of anti-tumor properties of Val-boropro in relation to inflammasome signaling

by

Saskia Hartner, BSc

Internal Supervisor: Pavel Kovarik, PhD

External Supervisor: Richard A. Flavell, PhD, FRS



AUSTRIAN
MARSHALL PLAN FOUNDATION
VIENNA | AUSTRIA



Howard Hughes
Medical Institute

Acknowledgments

I want to thank the Austrian Marshall Plan Foundation for supporting my studies through a generous scholarship. All experiments shown in this study were performed in collaboration with Dr. James Brewer, who I want to thank for being a great mentor, teacher and friend. I am grateful to Dr. Richard A. Flavell for the opportunity to work and learn in his Laboratory at the Yale School of Medicine as well as my supervisor at the University of Vienna Dr. Pavel Kovarik. I also want to thank Dr. Michael Chiorazzi, Holly Steach, Matthias Skadow, Dr. Autumn York, Dr. Ruaidhri Jackson Dr. Walter Mowel, Abigail Jarret, Dr. Manoulis Roulis, Laura-Sophie Frommelt, Linda Evangelisti, Patty Raney, Cindy Hughes, Elizabeth Hughes-Picard, Dave Urbanos, Jon Alderman, Caroline Lieber and all Flavellians for their great advice and help. My family, friends and especially my husband who always support and encourage me in my studies have my deepest gratitude.

Table of Contents

1	List of Abbreviations	4
2	Abstract.....	6
3	Introduction	7
4	Materials and Methods	11
4.1	Mouse models.....	11
4.2	Cell Lines	11
4.3	Reagents.....	11
4.4	Tumor growth curve models	11
4.5	Flow cytometry	11
4.6	Immunohistochemistry	12
4.7	Neutrophil Depletion Experiments	12
4.8	SDS polyacrylamide gel electrophoresis and Western Blot analysis.....	13
4.9	qPCR	13
5	Results	15
6	Discussion.....	25
7	Table of Figures	27
8	References.....	28

1 List of Abbreviations

AIM2	absent in melanoma 2
AOM-DSS	azoxymethane-dextran sulfate sodium
ASC	apoptosis-associated speck like protein containing a CARD
CARD	caspase activation and recruitment domain
CAR	chimeric antigen receptor
Casp1	caspase-1
CTL	cytotoxic T cell
CTLA-4	cytotoxic T-lymphocyte associated antigen 4
CXCL	chemokine motive ligand
DAMP	danger associated molecular pattern
DMEM	Dulbecco's Modified Eagle Medium
DPBS	Dulbecco's phosphate buffered saline
DPP	dipeptidyl peptidase
EDTA	ethylenediaminetetraacetic acid
ENU	N-ethyl-Nnitrosourea
FAP	fibroblast activating protein
FasL	Fas ligand
FBS	fetal bovine serum
FIIND	function to find domain
GSDMD	gasdermin D
IFN	interferon
IL	interleukin
IL1R	interleukin 1 receptor
LF	lethal factor
LRR	leucine rich repeats
MDSC	myeloid derived suppressor cell
NBD	nucleotide binding domain
NK cell	Natural killer cell
NLR	NOD-like receptor
NLRC	NOD-, LRR- and CARD containing protein
NLRP	NOD-, LRR- and PYD containing protein
P/S	penicillin/streptomycin
PAMP	pathogen associated molecular pattern
PBS-T	phosphate buffered saline, 0.1% Tween
PD-1	programmed death protein 1
PMA	phorbol 12-myristate 13-acetate
Polr2a	RNA Polymerase II subunit A
Pro-casp1	pro-caspase-1
PVDF	Polyvinylidene difluoride
PYD	pyrin domain
qPCR	quantitative polymerase chain reaction
RPMI	Roswell Park Memorial Institute Medium

SDS sodium dodecyl sulfate
SDS PAGE sodium dodecyl sulfate polyacrylamide gel electrophoresis
SEM standard error of mean
T cells thymus dependent lymphocytes
TGF- β transforming growth factor β
Th1 cell T helper cell
TLR Toll-like receptor
VBP Valboro-Pro
WT wild type
YUMMER1.7 Yale University mouse melanoma cell line 1.7 exposed to radiation

2 Abstract

Immunotherapy is one of the biggest breakthroughs in cancer of the last decades (Couzin-Frankel 2013). It has revolutionized the way we think about and treat cancer. Many patients have already benefited from this treatment. A commonly used form of immunotherapy, targets so called “immune-checkpoints” in cancer patients. These checkpoints prevent chronic stimulation of T cells during immune responses and are important for self-tolerance, but also lead to a reduced T cell response to cancer (Ribas and Wolchok 2018). Checkpoint inhibitors, like the monoclonal antibodies Ipilimumab and Nivolumab target CTLA-4 and PD-1 respectively, blocking the immune checkpoints that would otherwise lead to a reduced T cell response (Pardoll 2012). Unfortunately, only a subset of cancer patients responds to immunotherapy. Additionally, some patients receiving immunotherapeutics experience severe adverse effects. To overcome these caveats new strategies need to be developed. Most of the currently used approaches target the adaptive immune system. The role of the innate immune system in anti-tumor immunity requires further research in order to be effectively targeted through immunotherapies. The inflammasome is a promising innate immune target and might be utilized for developing new therapies, as inflammasome activation has been shown to induce anti-tumor immunity (Yao et al. 2017). Furthermore, the pro inflammatory cytokine IL-18 that is released upon inflammasome activation, is a known IFN γ inducer in Th1 cells and can activate cytotoxic T cells (CTLs) and NK cells and therefore enhances tumor immunity (Esmailbeig and Ghaderi 2017; Bohn et al. 1998).

In this study we present that stimulation of the innate immune sensor Nlrp1 through the amino-boronic dipeptide Valboro-Pro (VBP) leads to anti-tumor immunity in mice. We further unraveled the crucial role of Casp1 and its substrate, the pro inflammatory cytokine IL-18 in VBP induced tumor growth suppression. Although the exact working mechanism of VBP is still unknown, we shed light to the cellular response mediating VBP induced anti-tumor immunity. Our work lays path for development of new immunotherapies targeting the inflammasome, which might be used in combination with currently used treatment strategies to improve and enhance anti-tumor immunity in patients.

3 Introduction

Cancer arises from abnormally proliferating cells, showing hallmarks of resistance to cell death, evasion of growth suppressors, induction of angiogenesis, invasion and metastasis (Hanahan and Weinberg 2011). The underlying processes that foster the development of cancer are genomic instability as well as inflammation (Negrini et al. 2010; Colotta et al. 2009; Qian and Pollard 2010). The immune system is in principle capable of controlling tumor development through cytotoxic innate and adaptive immune cells. Some cancer cells are however capable of evading immune detection or killing and are therefore able to persist and grow into tumors (Gonzalez et al. 2018; Steer et al. 2010; Schietinger et al. 2008). Recent efforts to understand why cancer cells are not recognized or killed by the immune system lead to breakthroughs in the development of cancer immunotherapies that activate or reactivate the immune system to recognize and kill cancer cells. During a response to cancer, activated T cells upregulate the negative regulatory receptor PD-1 and the negative regulator of costimulation CTLA-4, which induce immunosuppression (Ribas and Wolchok 2018). These molecules are considered immune checkpoints, as they prevent chronic stimulation and are essential for self-tolerance (Chamoto et al. 2017). Monoclonal antibodies like Nivolumab and Ipilimumab are used to target these checkpoints in order to block immunosuppression, resulting in a continuous T cell response against cancer cells (Pardoll 2012; Wolchok et al. 2017). These forms of immunotherapies are called Checkpoint inhibitors. Another immunotherapeutic strategy to treat cancer are chimeric antigen receptor (CAR) T-cells. Here, T cells are collected from patients, genetically modified to express synthetic chimeric antigen receptors specifically targeting cancer cells and transferred back into respective patients (Gomes-Silva and Ramos 2018). These therapies however, often result in unacceptable adverse effects, such as autoimmunity, toxicity (cytokine release syndrome, neurotoxicity, fever, etc.) or resistance to therapy (Savoia et al. 2016; Badieyan and Hoseini 2018; Zaretsky et al. 2016).

Most of the current immunotherapies are acting on or utilizing the adaptive immune system (Galon and Bruni 2019; Tumeh et al. 2014), while the role of the innate immune system in tumor killing is less understood and has only recently become an emphasized research target (Woo et al. 2014; Marcus et al. 2014; Chow et al. 2019). In order to utilize the innate immune system for cancer immunotherapy, it is crucial to understand the role of innate immune cells in the tumor microenvironment. Multiple reports on myeloid derived suppressor cells (MDSCs) show a tumor growth promoting effect of this cell type (Dominguez et al. 2017; Gabilovich 2017). Some myeloid derived immune cells of the tumor microenvironment, such as macrophages can be polarized toward tumor growth suppressive or tumor growth promoting effector functions (Colegio et al. 2014; Zhang et al. 2014; Ohri et al. 2009). Recent studies implicate that such tumor promoting or suppressing polarization can also be observed for tumor associated neutrophils. TGF- β has been identified as the factor polarizing neutrophils to a tumor growth promoting phenotype (Shaul and Fridlender 2017; Fridlender et al. 2009). Neutrophils have been shown to promote breast cancer

metastasis through inhibition of CD8 T-cell function (Coffelt et al. 2015). Other studies have demonstrated an involvement of neutrophils driving unconventional T cell mediated tumor resistance in mouse and human sarcomas. (Ponzetta et al. 2019). These studies demonstrate the dual role of neutrophils in tumor growth suppression or tumor growth promotion.

It was previously shown that antigen specific cytotoxic T cells (CTLs) feedback to antigen presenting cells (APCs), leading to Nlrp3 activation, IL-1 β maturation and ultimately induced antigen specific anti-tumor immunity (Yao et al. 2017). The pro inflammatory cytokine IL-18 released upon inflammasome activation, is known to induce the effector molecule IFN γ in Th1 cells. Furthermore, it can activate cytotoxic T cells (CTLs) and NK cells and therefore lead to enhanced tumor immunity (Esmailbeig and Ghaderi 2017; Bohn et al. 1998). Further research is however required to better understand how the innate immune system can be exploited for cancer immunotherapy. One promising target might be the inflammasome.

Inflammasome are multimolecular, intracellular complexes that form upon activation of innate inflammasome immune sensors, recognizing microbial and endogenous damage-associated molecular patterns (DAMPs) as well as pathogen-associated molecular patterns (PAMPs). Therefore, inflammasome sensors are so called pattern recognition receptors and consist of the family members AIM2, NLRC4 (NOD-, LRR- and caspase activation and recruitment domain-containing) protein 4, NLRP1 (NOD-, LRR- and pyrin domain-containing) protein 1, NLRP3, NLRP6 and PYRIN (Malik and Kanneganti 2017). They typically consist of a nucleotide-binding domain, leucine-rich repeat containing proteins (NLR or NOD like receptor) or absent in melanoma 2-like receptors (AIM2-like receptors). Canonical inflammasome signaling occurs in two steps: First, toll-like receptors (TLR), NOD1 or NOD2 are activated through recognition of DAMPs, PAMPs or other stimuli, leading to NF- κ B signaling and subsequent mRNA and protein expression of pro-IL1 β and pro-IL18. (Kolb et al. 2014; Chen and Nunez 2011). Next, inflammasome sensor mediated recognition of danger signals leads to oligomerization and recruitment of pro-Casp1 to the inflammasome complex. Ligand activated inflammasome sensors can either interact with and recruit pro-Casp1 through a caspase activation and recruitment domain (CARD) or through an adaptor protein, like the apoptosis-associated speck-like protein containing a caspase recruitment domain (ASC) (Schroder and Tschopp 2010; Di Virgilio 2013). ASC consists of a pyrin domain (PYD) and a caspase recruitment domain (CARD), allowing ASC to bridge the inflammasome sensor molecule to pro-Casp1 via CARD-CARD interactions. Pro-Casp1 is then cleaved into its activated form Casp1 through proximity induced autoproteolytic cleavage (Broz and Dixit 2016), allowing cleavage of pro-IL1 β and pro-IL-18 into their active, proinflammatory forms (Kolb et al. 2014; Di Virgilio 2013). In addition to the cytokines IL-1 β and IL-18, gasdermin D (GSDMD) is another substrate of caspase-1. GSDMD is a pore forming protein, which enables the release of the cytokines through a lytic form of cell death, called pyroptosis (Shi et al. 2015). Induction of pyroptosis and the release of the cytokines IL-1 β and IL-18 ultimately leads to inflammation.

As innate immune sensors, inflammasomes and their signaling pathways became promising targets for cancer immunotherapy. They have been shown however to play diverse and sometimes even contradicting roles in cancer promotion and therapy. Differences in these inflammasome mediated responses are due to context, as the tissue of inflammasome activation, microbial products or the cancer cells themselves can contribute (Karki et al. 2017). Furthermore, the cytokines IL-1 β and IL-18 are associated with distinct functions in tumor immunity. IL-1 β has been shown to be involved in promotion of tumor growth. A study by Novartis suggests, that inhibition of IL-1 β through the monoclonal antibody canakinumab leads to a significant reduction in the incident of all fatal cancers (Ridker et al. 2017). Other studies showed promotion of inflammation and tumorigenesis of gastric cancer through IL-1 β (Tu et al. 2008; Li et al. 2012), confirming the tumor promoting role of IL-1 β . IL-18 on the other hand has been shown to be associated with anti-tumor immunity by multiple studies. Mice deficient in IL-18 show an increase in inflammation and tumorigenesis in azoxymethane/dextran sodium sulphate (AOM/DSS) induced colitis-associated colon cancer (Salcedo et al. 2010; Zaki et al. 2010). In murine MC38 colorectal liver cancer, IL-18 leads again to tumor growth suppression, through induction of NK cell maturation and priming of their tumoricidal function in a FasL-sensitive tumor cell dependent matter (Dupaul-Chicoine et al. 2015). These studies highlight the tumor growth inhibitory properties of IL-18.

In this thesis we focus on the Nlrp1 inflammasome as a potential cancer immunotherapy target. Human NLRP1 consists of an N-terminal pyrin domain (PYD), a nucleotide binding domain (NBD), a leucine-rich repeat domain (LRR), a function to find domain (FIIND) and a C-terminal caspase activating and recruitment domain (CARD). Mouse Nlrp1 is similar to human NLRP1, but lacks the PYD domain (Franchi et al. 2012). Autolytic proteolysis in the FIIND domain is required for NLRP1 activation and human NLRP1 depends on ASC for Casp1 recruitment, while mouse *Nlrp1* can also interact directly with capase-1 through its CARD domain (Finger et al. 2012; Chavarria-Smith and Vance 2015). Mouse *Nlrp1* has undergone at least two gene duplications, leading to the paralogs *Nlrp1a*, *Nlrp1b* and *Nlrp1c*. Furthermore, there are at least five allelic variants in different inbred mouse strains for *Nlrp1b* (Boyden and Dietrich 2006). *Nlrp1c*, lacking a card domain, is a predicted pseudogene is not known to form a functional inflammasome. The *Nlrp1a*^{Q593P/Q593P} gain of function mutation leads to a constitutively activated inflammasome in mice, resulting in severe auto inflammation, with neutrophil counts elevated 15 fold compared to wild type. This mutation was found through an N-ethyl-Nnitrosourea (ENU) mutagenesis screen for dominant neutrophilia inducing mutations (Masters et al. 2012). In addition to the hematopoietic compartment, NLRP1 is also highly expressed in skin (Zhong et al. 2016). While there are no reported stimuli for Nlrp1a activation, different alleles of Nlrp1b in various mouse strains can be activated by *bacillus anthracis* lethal factor (LF), *Toxoplasma gondii* and ATP depletion (Chavarria-Smith and Vance 2015). The nonselective inhibitor of post-proline cleaving serine proteases Val-boroPro (VBP) was

recently shown to activate Nlrp1 through inhibition of the dipeptidyl peptidases Dpp8 and Dpp9 (Okondo et al. 2017; Gai et al. 2019). In addition to Dpp8 and Dpp9, VBP inhibits other S9 family members as Dpp4, Dpp7 and the fibroblast activating protein FAP (Okondo et al. 2017). Even though the mechanism of Dpp8/9 inhibition leading to Nlrp1b activation is not yet uncovered, this finding was a major step in understanding the working mechanism of VBP. Studies predating this finding, already showed that VBP induces a powerful anti-tumor immune response in syngeneic mouse models. Tumors of mice subcutaneously injected with different syngeneic murine cancer cell lines, like B16-F10 melanoma, EL4 lymphoma cells or WEHI 164 fibrosarcoma cells, showed severe growth inhibition upon treatment with VBP (Adams et al. 2004). The observed anti-tumor immunity induced by VBP, depends on the adaptive immune system with a crucial role of T cells (Adams et al. 2004; Walsh et al. 2013).

The aim of this thesis is to further illuminate the working mechanism of VBP, investigating the response leading to tumor growth suppression. We will test if VBP induced anti-tumor immunity depends on Nlrp1 signaling and the involvement of the pro-inflammatory cytokines IL-1 β and IL-18. Furthermore, we will investigate the cellular response to VBP with the purpose of identifying the immune cell subsets that are important for tumor growth inhibition. Tumor growth curve experiments using syngeneic tumor models in wild type mice and mice deficient in various components of inflammasome signaling will shed light to the involvement of Nlrp1 signaling in VBP induced tumor growth inhibition. To interrogate cell subsets involved in VBP mediated tumor growth inhibition we will analyze tissue, like tumor or tumor draining lymph nodes through flow cytometry. These experiments will reveal possible effector cell subsets give implications about putative cell interactions of the innate and adaptive immune system. Taken together, we want to elucidate pathways leading to anti-tumor immunity, providing new targets that can be used in cancer immunotherapy.

4 Materials and Methods

4.1 Mouse models

Mice on the C57BL/6 background were used in all *in vivo* experiments. *Nlrp1*^{-/-} mice were previously described (Kovarova et al. 2012) and purchased from the Jackson Laboratories (#021301). *Casp1*^{-/-} were previously described (Case et al. 2013) and maintained by the Flavell Laboratory. *IL18*^{-/-} and *IL1R*^{-/-} were previously described (Takeda et al. 1998; Glaccum et al. 1997) and purchased from the Jackson Laboratories (#004130, #003245). All mice were bred and maintained in specific pathogen-free conditions and in accordance with Yale Institutional Animal Care & Use Committee.

4.2 Cell Lines

Yale university mouse melanoma cells 1.7 (Yummer1.7) have been described previously and were kindly provided by Marcus Bosenberg (Dermatology Department, Yale School of Medicine) (Wang et al. 2017). Yummer1.7 cells were cultured in DMEM F12 (1:1), supplemented with 10% FBS and 100 µg/ml Penicillin Streptomycin (P/S). The mouse colorectal cancer cell line MC38 has previously been described and was kindly provided by Marcus Bosenberg (Dermatology Department, Yale School of Medicine). MC38 cells were cultured in DMEM supplemented with 10% FBS and 100 µg/ml Penicillin Streptomycin.

4.3 Reagents

Valboro-Pro (VBP; Talabostat mesylate, MedKoo Biosciences) was dissolved in 0.1M HCl and diluted with 0.9% NaCl to a final concentration of 20µg/150µl, used to gavage mice. As vehicle control 0.9% NaCl with 0.001M HCL was used to gavage mice.

4.4 Tumor growth curve models

9-12 week old mice were subcutaneously injected with 5x10⁶ Yummer1.7 or 0.5x10⁶ MC38 cells, suspended in 100 µl Dulbecco's PBS (DPBS). In order to control for effects caused by diverging microbiota, mice of different genotypes and/or different treatments were cohoused. For tumor growth curve experiments, 20µg of VBP were administered p.o. through gavage twice daily. Tumor sizes were assessed by measuring the greatest length and width, using a caliper. Tumor volumes were calculated using the formula: Tumor volume=width²x0.5xlenght. VBP treatment was started at day 2 for Yummer1.7 tumors and day 7 for MC38 growth curves. Mice were assigned to Vehicle or VBP group before tumor inoculation for Yummer1.7. For MC38, tumor sizes were calculated on day 7 before treatment to ensure experimental groups were size matched.

4.5 Flow cytometry

For flow cytometry experiments of the blood, mice were i.v. injected with 100µg VBP. 50ul blood was collected though retro orbital bleed 6 hours after injection using

heparinized capillaries and tubes. Blood was stained with antibodies (concentration 1:150) in FACS buffer (1% Calf serum in DPBS with 1 mM EDTA), on ice for 30 min. 3ml of RBC Lyse/Fix/Wash (Biolegend) was added to blood samples and incubated at room temperature for 10 min. After centrifuging cells were washed, resuspended in FACS buffer and analyzed on a Cytoflex. For tumor flow cytometry experiments, 0.5 million MC38 or 5 million Yummer1.7 cells were subcutaneously injected into mice. Treatment with 20µg VBP or vehicle was started 7 days after injection and continued for a week. On day 14 mice were sacrificed and tumors were collected. Tumors were minced using a razor blade in RPMI with Collagenase D (1:100) and DNase (1:1000), further disassociated using gentleMACS Dissociator (MACS Miltenyi Biotec) and afterwards incubated in a shaker at 37°C for 45 minutes. Next, tumors were pushed through a 100µm cell strainer and if necessary, resuspended in 10 ml of ACK Buffer to lyse red blood cells. Cells were washed with FACS Buffer and resuspended in an appropriate volume of FACS buffer, depending on cell pellet size. For intracellular staining of cytokines, cells were stimulated with PMA (20-50ng/ml) and ionomycin (1mM), and incubated for a total of 4 hours at 37°C. After two hours Brefeldin A (Biolegend, #420601) was added. For staining of cell surface markers or intracellular staining that does not involve cytokine staining, no PMA ionomycin stimulation and treatment with Brefeldin A is needed and these steps should be skipped. Afterwards, cells were pelleted and resuspended in 5% Rat serum to block unspecific antibody binding. After a wash with FACS buffer, cells were stained with fluorochrome-conjugated antibodies in FACS buffer (1:300) and incubated for 30 minutes on ice in the dark. Cells were washed with DPBS twice and incubated with fixable viability dye in DPBS (1:500) for 15 minutes on room temperature in the dark, to stain for dead cells. Next, cells were washed 2x with DPBS and fixed in 4% PFA in DPBS for 15 minutes on ice. After two washes with FACS buffer, cells were resuspended in FACS buffer and filtered through an 80µm filter and analyzed on an LSR2 or a Cytoflex.

4.6 Immunohistochemistry

For immunohistochemistry mice were subcutaneously injected with 5 million Yummer1.7 cells. Mice were euthanized one week after injection and tumors were collected, fixed in 10% NBF overnight. Tumors were then transferred to 70% Ethanol and embedded in paraffin. Sections of the tumors were stained with Ly6G by HistoWiz (<https://home.histowiz.com/>).

4.7 Neutrophil Depletion Experiments

For depletion experiments using anti-Ly6G antibody, mice were injected with 50µg anti-Ly6G (BioXcell, #BE0075-1) or anti-IgG (BioXcell, #BE0089) control antibody i.p. and 3 days later injected with 5 million Yummer1.7 cells subcutaneously. 100µg of anti-Ly6G or anti-IgG control was then administered every 3 days, starting on the injection day of Yummer1.7 for a total of 4 treatments. Mice were gavaged with 20µg of VBP or vehicle 2x/daily starting 2 days after Yummer1.7 cell injection, until mice were sacrificed on day 11 after Yummer1.7 cell injection. Tumor volume was measured 2x a week using a caliper.

For depletion experiments using anti-Ly6G antibody in combination with a secondary anti-rat antibody (Faget et al. 2018), mice were injected with 0.5 million MC38 cells. A week after tumor cells injection, mice were injected i.p. with 100µg anti-Ly6G (BioXcell, #BE0075-1) or anti-IgG (BioXcell, #BE0089) control antibodies. Together with the start of antibody administration (Day 1), treatment with 20µg of VBP or vehicle 2x/daily through gavage was started and continued for 2 weeks, when the experiment was ended. On day 2 mice previously treated with anti-Ly6G antibody, were injected with 100µg secondary anti-rat Kappa antibody (Bioexcell, #BE0122). Mice were administered anti-Ly6G antibody on day 3, and anti-IgG antibody on day 4. On day 6 mice previously treated with anti-Ly6G antibody were injected with secondary anti-rat Kappa antibody. Mice were injected with anti-Ly6G antibody and anti-IgG antibody on day 7, respectively, followed by injection of secondary anti-rat antibody on day 8. Mice were bled the next day to validate the depletion efficiency through flow cytometry. The antibody treatment schedule (days 1-8) was repeated once for a total of 2 weeks.

4.8 SDS polyacrylamide gel electrophoresis and Western Blot analysis

Yummer1.7 or MC38 cells respectively, were stimulated with 10ng/ml IL-1β for 0, 5, 10, 30, 60 or 240 minutes in DMEM or DMEMF12. Whole cell extracts were collected through lysis with NP40 lysis buffer and protein content was quantified using a BSA standard curve (DC™ Protein Assay, BioRad). Equal amounts of protein per sample were separated under reducing conditions on a 4-12% Bis-Tris Polyacrylamide Gel (Invitrogen, # NP0322BOX) in 1x NuPAGE MOPS SDS Running buffer (Invitrogen, #NP0001) at 130V. Protein was then electrophoretically transferred onto a methanol activated polyvinylidene fluoride (PVDF) membrane and equilibrated in 1x NuPAGE Transfer Buffer (Invitrogen) with 10% methanol for 2h at 120V and 4°C. Next, the membrane was blocked in 5% milk for 5 minutes. Afterwards the PVDF membrane was incubated with anti-Ikβα primary antibody (cell signaling 9242S, 1:1000) in 5% milk overnight at 4°C, followed by two washes in PBS-T. Then the secondary anti-rabbit IgG Horseradish Peroxidase linked whole antibody (ECL™, #NA9340V) was added to 5% milk (antibody concentration 1:2000) and incubated for 1-3 hours at room temperature. The PVDF membrane was then washed 2x with PBS-T and signal was detected with SuperSignal™ West Pico or Femto Chemiilluminescent Substrate (Thermo Fisher) on a ChemiDoc™ MP Imaging System (BioRad). Membrane was washed with PBS-T 2x for 5 minutes and incubated with anti-beta Tubulin (E7, DSHB) in 5% milk (antibody concentration 1:2500) for 1 hour at room temperature, used as a loading control. After another 2 washes with PBS-T (5 minutes each), the membrane was incubated with secondary anti-mouse IgG Horseradish Peroxidase linked whole antibody (ECL™, #NA931V) for 1-2 hours. The PVDF membrane was then washed 2x with PBS-T and signal was detected with SuperSignal™ West Pico or Femto Chemiilluminescent Substrate (Thermo Fisher) on a ChemiDoc™ MP Imaging System (BioRad).

4.9 qPCR

Yummer1.7 or MC38 cells respectively, were stimulated with 10ng/ml IL-1β for 0, 5, 10, 30, 60 or 240 minutes in DMEM or DMEMF12. RNA was extracted through cell

lysis with Trizol. After RNA purification, cDNA was synthesized using SuperScript™ II Reverse Transcriptase Kit (Invitrogen™, #18064014) following the manual provided by the manufacturer. Reaction mix, using Primers for Cxcl1, Cxcl2 and the housekeeping gene Polr2a, was run on a C100 Touch™ Thermal Cycler (CFX96™ Real-Time System, Biorad) was run under following conditions:

Primer	Sequence
Cxcl1 Forward	5'-AAAGATGCTAAAAGGTGTCC
Cxcl1 Reverse	5'-GTATAGTGTTGTCAGAAGCC
Cxcl2 Forward	5'-GGGTTGACTTCAAGAACATC
Cxcl2 Reverse	5'-CCTTGCCTTTGTTCAGTATC
Polr2a Forward	5'-CGGTTGAATCTTAGTGTGAC
Polr2s Reverse	5'-ATAGCCAACCTCTTGGATCTC

reaction mix	[μl]
cDNA	1
Primer F (100 μ m)	0.05
Primer R (100 μ m)	0.05
Sybr	5
H ₂ O	3.9

40x { 95°C 3min
 95°C 10s
 55°C 30s

Melt curve 65°C to 95°C, Celsius increment 0.5°C (5s)

5 Results

As previously shown, VBP can induce a powerful anti-tumor immune response (Adams et al. 2004; Walsh et al. 2013). The mechanism leading to tumor growth inhibition is however only poorly understood. To investigate if the working mechanism of VBP induced anti-tumor immunity depends on the Nlrp1 inflammasome, we performed tumor growth curve experiments. Syngeneic Yumner1.7 cells were injected subcutaneously into Nlrp1^{-/-} and Nlrp1^{+/+} (Control) C57BL/6 mice, treated with VBP or vehicle, respectively. Tumor growth was monitored for a period of 8 weeks. We observed complete tumor rejection in all control mice treated with VBP, whereas tumors in Nlrp1^{-/-} mice treated with VBP, grew out (Fig. 1A). Tumors of mice treated with vehicle grew out as well, regardless of their genotype (Fig. 1B). These results are also reflected in the overall survival, with 100% survival of Nlrp1^{+/+} mice up to 8 weeks, whereas Nlrp1^{-/-} mice treated with VBP or vehicle treated mice, die between 3 and 6 weeks (Fig.1C). We observed an impaired response to VBP in Nlrp1^{+/+} mice (data not shown) and tested whether this is due to haploid insufficiency, by monitoring neutrophil mobilization following VBP treatment. Indeed, VBP induced only an intermediate increase in circulating neutrophils in Nlrp1^{+/+} mice, compared to WT or Nlrp1^{-/-} mice upon single dose treatment of VBP (Fig.1D,E). Therefore, Nlrp1 expression might not be sufficient in Nlrp1^{+/+} mice to efficiently suppress tumor growth in response to VBP treatment. These results suggest that VBP induced anti-tumor immunity depends on Nlrp1.

Next, we tested whether the Nlrp1 is functioning as an inflammasome sensor in our model. We therefore assessed if Casp1, which is recruited to Nlrp1 upon activation to form the inflammasome, is required for VBP induced tumor growth inhibition. We therefore, monitored Yumner1.7 tumor growth in Casp1^{-/-} or WT and Casp1^{+/+} C57BL/6 mice, referred to as control mice, that were either administered VBP or vehicle. Casp1^{-/-} mice treated with VBP, failed to suppress tumor growth, while in 13 out of 17 control mice treated with VBP, we could observe tumor remission and tumor rejection (Fig. 1F). Tumors of vehicle treated mice grew out, regardless of their genotype (Fig. 1G). However, 3 out of 18 Casp1^{-/-} mice treated with VBP and 1 mouse out of 15 Casp1^{-/-} mice treated with vehicle never grew out tumors. We believe, that this can be interpreted as background, due to variation in cancer cell injection which can influence the ability of injected cells to form viable tumors. Casp1^{-/-} mice treated with VBP and vehicle treated mice had significantly lower survival rates than control mice treated with VBP (Fig.1H). Overall, these findings confirm a crucial role of Casp1 in VBP induced anti-tumor immunity.

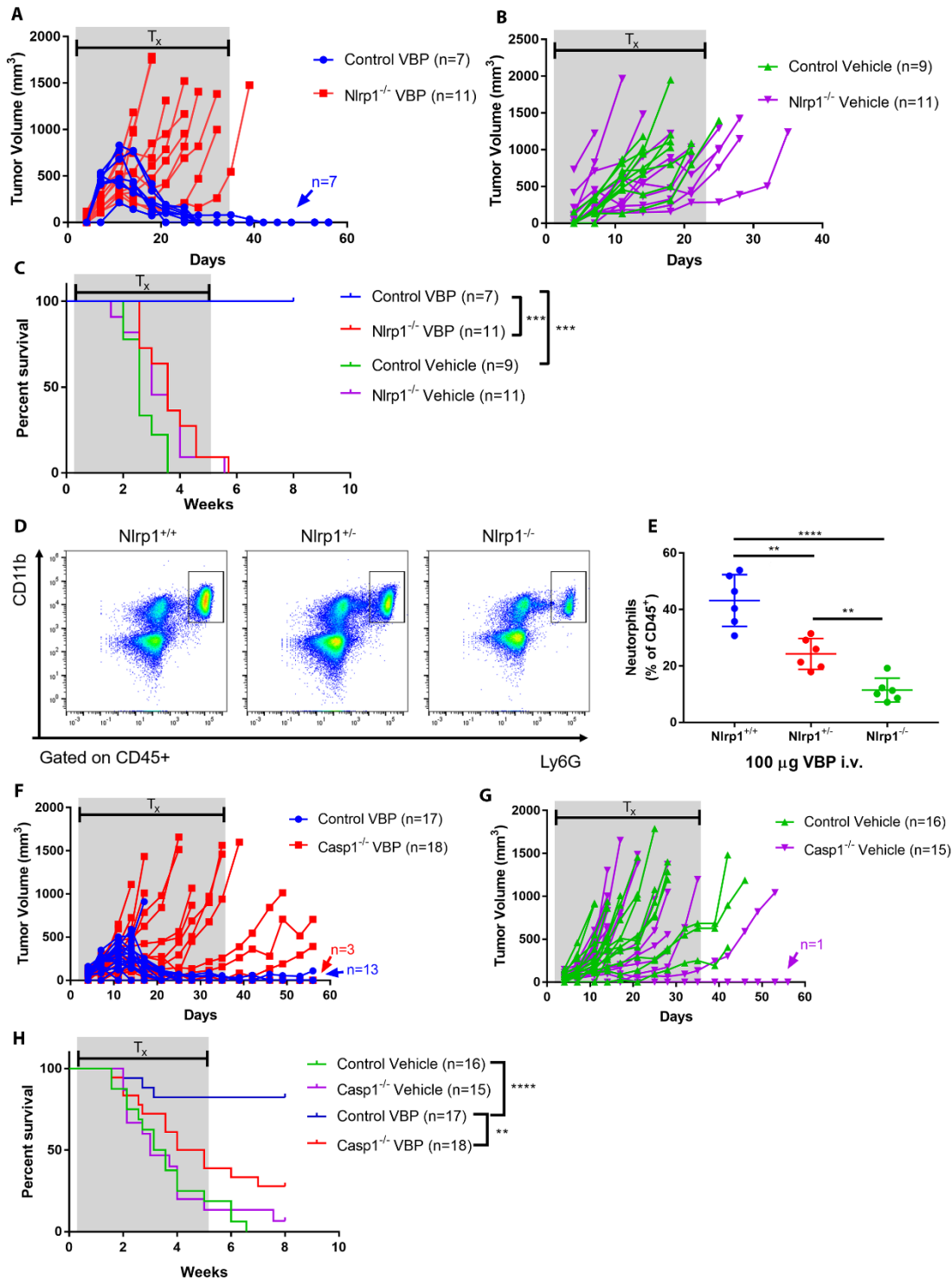


Fig. 1: VBP induced anti-tumor immunity depends on the Nlrp1 inflammasome

A,B Yumner1.7 cells injected in Nlrp1^{+/+} and Nlrp1^{-/-} C57BL/6 mice at day 0, VBP (20µg) or vehicle treatment (T_x) started 2 days after injection and administered 2x/day p.o. over 5 weeks. Tumor growth was monitored through tumor measurements 2x/week. Data was pooled from two individual experiments. **C** Survival analysis of mice from experiment A and B. Log-rank (Mantel-Cox) test, $p=0.1234$ (ns), $p=0.0332$ (*), $p=0.0021$ (**), $p=0.0002$ (***), $p<0.0001$ (****) **D** Representative Flow cytometry analysis of neutrophils in circulation from Nlrp1^{+/+} (n=6), Nlrp1^{+/-} (n=6), Nlrp1^{-/-} (n=6) mice after a single dose of VBP. **E** Quantification of neutrophils in percentage to CD45⁺ from Nlrp1^{+/+} (n=6), Nlrp1^{+/-} (n=6), Nlrp1^{-/-} (n=6) C57BL/6 mice after a single dose of VBP. Significance was calculated using an unpaired t-test, $p=0.0014$ (**), $p=0.0001$ (****) **F,G** 5 million Yumner1.7 cells injected in Casp1^{+/+} and Casp1^{-/-} (Control) or Casp1^{-/-} C57BL/6 mice at day 0, VBP (20µg) or vehicle treatment (T_x) started 2 days after injection and administered 2x/day p.o. over 5 weeks. Tumor growth was monitored through tumor measurements 2x/week. Data was pooled from two individual experiments. **H** Survival analysis of mice from experiment F and G, Log-rank (Mantel-Cox) test, $p=0.1234$ (ns), $p=0.0332$ (*), $p=0.0021$ (**), $p=0.0002$ (***), $p<0.0001$ (****).

As VBP leads to Nlrp1 mediated and Casp1 dependent anti-tumor immunity, the question emerged if the cytokines IL-1 β and IL-18 are responsible for tumor growth inhibition. These pro-inflammatory cytokines are released in response to Nlrp1 activation in a Casp1 dependent manner. We therefore performed tumor growth curve experiments with Yummer1.7 in IL-18^{-/-} or IL-18^{+/-} and WT C57BL/6 mice (here referred to as control mice), treated with VBP or vehicle. We detected impaired tumor growth suppression of IL-18^{-/-} mice treated with VBP compared to control mice (Fig.2A,B). Control mice treated with VBP had a survival rate of 60% over a period of 8 weeks, while IL-18^{-/-} mice treated with VBP or vehicle treated mice had very poor survival rates (Fig.2C). Taken together, these results revealed the pro-inflammatory cytokine IL-18 to be a crucial factor in VBP induced tumor growth suppression. To assess the role of IL-1 β in VBP mediated tumor growth inhibition in the Yummer1.7 model, we analyzed tumor growth in IL-1R^{+/+} and IL-1R^{-/-} (Control) C57BL/6 mice treated with VBP or given vehicle. These mice lack the IL-1 receptor and are therefore unable to react to IL-1 α or IL-1 β . Most IL-1R^{+/+} mice treated with VBP showed tumor rejection (6 out of 9). A third of the IL-1R^{-/-} mice treated with VBP also experienced complete tumor remission (Fig.2D). Tumors in the vehicle treated groups however, grew out (Fig.2E). While we observed significantly better survival in VBP treated mice compared to the vehicle treated group, we did not detect an IL-1R dependent difference in survival (Fig.2F). To see if our findings are applicable in other tumor models, we want to perform similar experiments in the MC38 model. Preliminary data suggests that VBP induces an anti-tumor response in MC38 (Fig.2G), making it a suitable model to test the involvement of the Nlrp1 inflammasome in tumor growth inhibition.

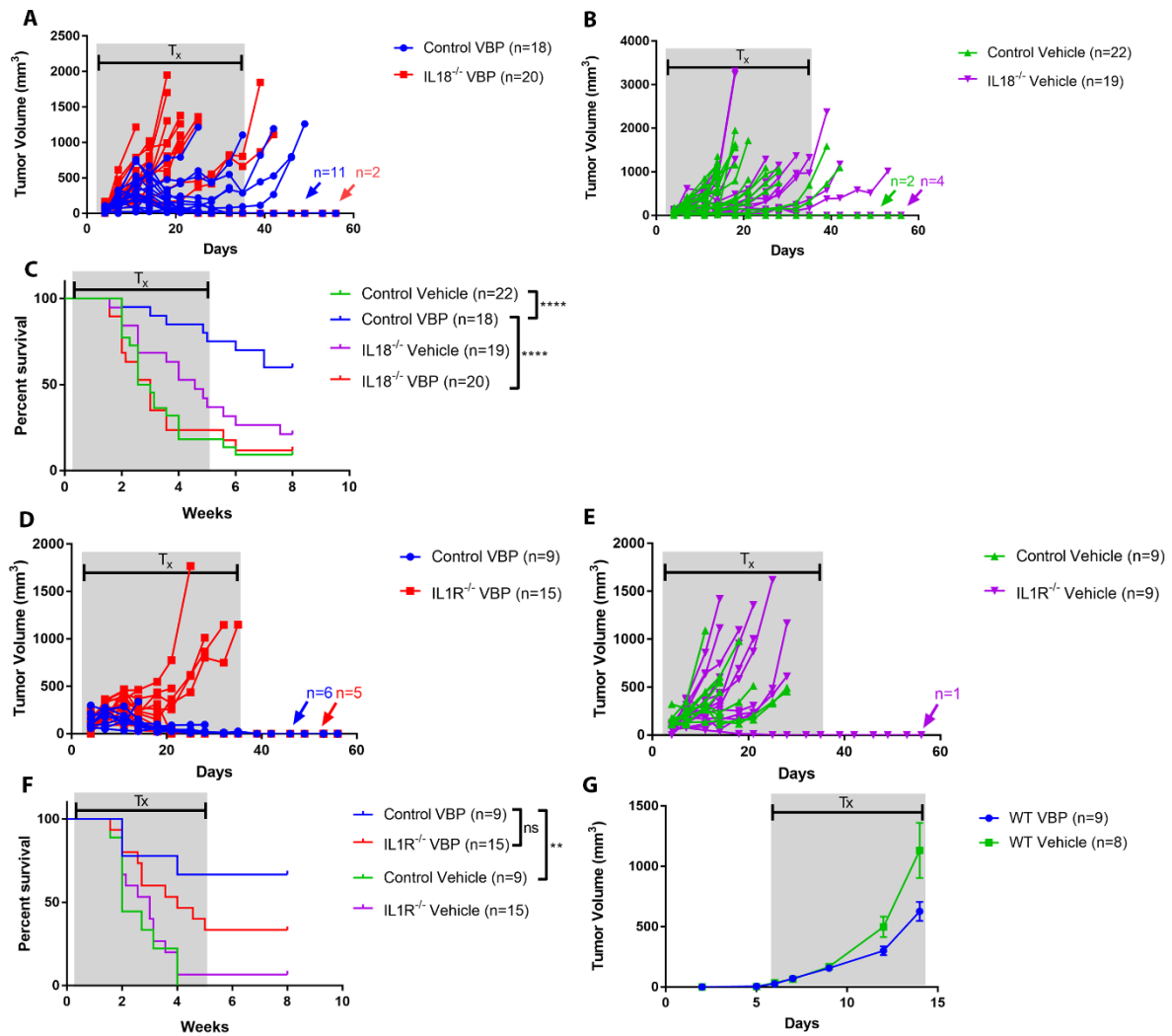


Fig. 2: IL-18 mediates VBP induced tumor growth suppression

A,B 5 million Yummer1.7 cells injected in IL-18^{+/+} and IL-18^{-/-} (Control) or IL-18^{-/-} C57BL/6 mice at day 0, VBP (20 μ g) or vehicle treatment (Tx) started 2 days after injection and administered 2x/day p.o. over 5 weeks. Tumor growth was monitored through tumor measurements 2x/week. Data was pooled from three individual experiments. **C** Survival analysis of mice from experiment A and B. Log-rank (Mantel-Cox), $p=0.1234$ (ns), $p=0.0332$ (*), $p=0.0021$ (**), $p=0.0002$ (***), $p<0.0001$ (****). **D,E** 5 million Yummer1.7 cells injected in IL-1R^{+/+} and IL-1R^{-/-} C57BL/6 mice at day 0, VBP (20 μ g) or vehicle treatment (Tx) started 2 days after injection and administered 2x/day p.o. over 5 weeks. Tumor growth was monitored through tumor measurements 2x/week. Data was pooled from two individual experiments. **F** Survival analysis of mice from experiment E and F. Log-rank (Mantel-Cox) test, $p=0.1234$ (ns), $p=0.0332$ (*), $p=0.0021$ (**), $p=0.0002$ (***), $p<0.0001$ (****). **G** 0.5 million MC38 cells were injected into WT C57BL/6 mice and grouped into treatment groups, based on Tumor size on day 7. VBP (20 μ g) and vehicle were administered 2x/daily p.o. from day 7 to Day 14 after injection and tumor growth was monitored through tumor measurement 3x/week. Error Bars indicate SEM.

A major outstanding question in the working mechanism of VBP, is the cellular response that mediates tumor growth inhibition. To investigate the presence and effector functions of innate immune cells in the tumor microenvironment, we performed flow cytometry on Yummer1.7 as well as MC38 tumors (Fig.3A). We observed an increase of tumor infiltrating neutrophils in Yummer1.7 tumors treated with VBP, compared to the vehicle treated group (Fig.3B,C). Additionally, Immunohistochemistry staining of VBP treated Yummer1.7 tumors show complete neutrophil infiltration, while neutrophils are only present in the periphery of Vehicle treated tumors (Fig.3C). To assess if the underlying mechanism of neutrophil recruitment involves the inflammasome, we analyzed tumor neutrophil infiltration of Nlrp1^{-/-} and Casp1^{-/-} mice compared to WT mice upon treatment with VBP through Flow Cytometry. A significant reduction in tumor infiltrating neutrophils (CD11b⁺, Ly6G⁺) was observed in the inflammasome knockouts Nlrp1^{-/-} and Casp1^{-/-}, confirming a dependence on the inflammasome in the recruitment of neutrophils to the tumor in the Yummer1.7 model (Fig.3E,F). Surprisingly, we did not find any infiltration of neutrophils in MC38 tumors treated with VBP. Neutrophil abundance was comparable in MC38 tumors of vehicle or VBP treated mice (Fig.3G,H). However, we detected an increase of neutrophils in the tumor draining lymphnodes of MC38 tumor bearing mice treated with VBP, suggesting that there is a systemic neutrophil expansion in this model, without successful tumor infiltration (Fig.3I,J). This observation suggests that Yummer1.7 cancer cells themselves might contribute to recruitment of neutrophils to the tumor. We detected that a key difference between Yummer1.7 cells and MC38 cells is their ability to respond to IL-1 β . While in Yummer1.7 cells IL-1 β stimulation leads to NF- κ B signalling, as I κ B α is degraded after 10 min of IL-1 β treatment, MC38 cells do not respond to IL-1 β (Fig.3K). Investigating the response of Yummer1.7 to IL-1 β at the expression level through qPCR, we found upregulation of the neutrophil chemoattractants Cxcl1 and Cxcl2 (Fig.3L). Hence, the ability of neutrophils to infiltrate tumors might rely on the presence of neutrophil chemokines in the tumor microenvironment, produced by certain cancers themselves.

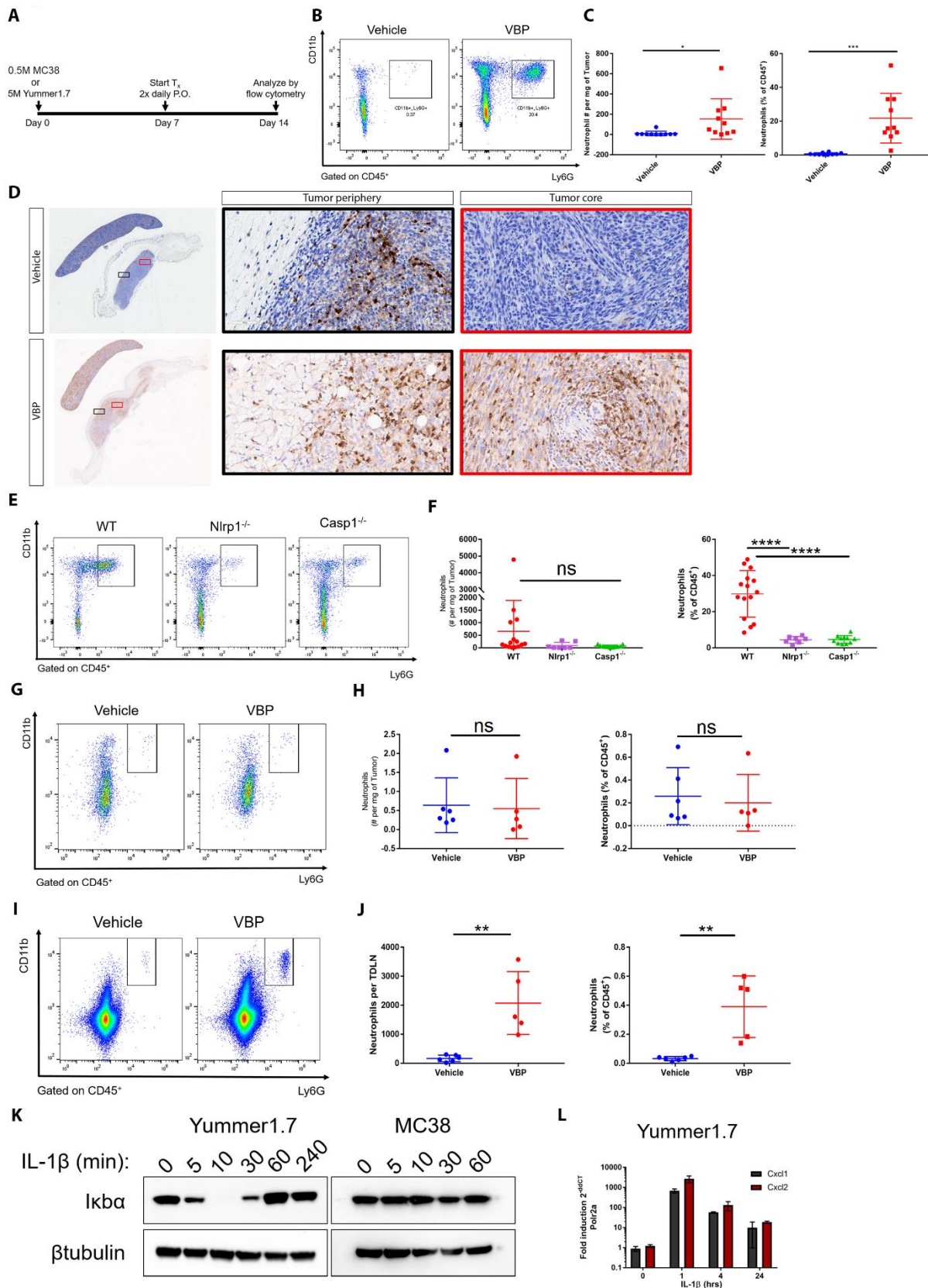


Fig. 3: VBP treatment leads to systemic neutrophilia

A Immunohistochemistry using anti-Ly6G antibody on spleen and Yummer1.7 tumor from VBP or vehicle treated WT C57BL/6 mice. **B** Experimental Outlay of Flow Cytometry experiments seen in C-J. Yummer1.7 or MC38 cells were injected into C57BL/6 mice. Treatment with VBP (20μg) or vehicle 2x/day p.o. was started on day 7 after injection and continued for a week. Mice were sacrificed on day 14 and tissue was analyzed through flow cytometry. **C** Representative flow cytometry data for CD11b⁺Ly6G⁺ cells in Yummer1.7 tumors from WT C57/BL6 mice treated with VBP or vehicle. **D** Quantification of CD11b⁺Ly6G⁺ as seen in C in total cell counts and percentage of CD45⁺

cells from Yummer1.7 tumors from WT C57/BL6 mice treated with VBP (n=10) or vehicle (n=10). Significance was calculated using an unpaired t-test, $p=0.0365$, $p=0.0003$. **E** Representative flow cytometry data of comparison of CD11b⁺Ly6G⁺ cells from Yummer1.7 tumors of WT, Nlrp1^{-/-} and Casp1^{-/-} upon VBP treatment. **F** Quantification of CD11b⁺Ly6G⁺ as seen in I in total cell counts and percentage of CD45⁺ cells from Yummer1.7 tumors of WT (n=15), Nlrp1^{-/-} (n=7) and Casp1^{-/-} (n=11) upon VBP treatment. Significance was calculated using an unpaired t-test, $p=2462$ (ns), $p<0.0001$. Data was pooled from two (Nlrp1) or three (Wt, Casp1) independently conducted experiments. **G** Representative flow cytometry data of CD11b⁺Ly6G cells from MC38 tumors of WT mice treated with VBP or vehicle. **H** Quantification of CD11b⁺Ly6G⁺ as seen in K in total cell counts and percentage of CD45⁺ cells from MC38 tumors of WT mice treated with VBP (n=5) or vehicle (n=6). Significance was calculated using an unpaired t-test, $p=0$. (ns) **I** Representative flow cytometry data of CD11b⁺Ly6G⁺ cells from MC38 tumor draining lymph node (TDLN) of WT mice treated with VBP or vehicle. **J** Quantification of CD11b⁺Ly6G⁺ as seen in M in total cell counts and percentage of CD45⁺ cells from MC38 tumor draining lymph node (TDLN) of WT mice treated with VBP (n=5) or vehicle (n=6). Significance was calculated using an unpaired t-test, $p=0.0019$. **K** Western Blot analysis of Yummer1.7 and MC38 cells after stimulation with IL-1 β for 0, 5, 10, 30, 60 or 240 minutes. Degradation of I κ b α is detected and β -tubulin is used as a loading control. **L** Cxcl1 and Cxcl2 detection through qPCR of Yummer1.7 cells stimulated with IL-1 β . Error bars indicate SD.

It was shown by previous studies that cells of the adaptive immune system and T cells in particular, are crucial for VBP induced tumor immunity (Adams et al. 2004; Walsh et al. 2013). To further investigate the role of T cells in our model, we used flow cytometry to assess T cell tumor infiltration in VBP compared to vehicle treated mice (Fig.4A). We did not detect any T cells in Yummer1.7 tumors treated with VBP or vehicle. The lack of T cell detection in this tumor model might however, underlie technical problems. One possible reason could be that the time point of tumor analysis with 2 weeks after injection is either too late or too early for T cell detection. We therefore decided to analyze tumor infiltrating T cells in MC38 tumor, as we also expect T cells to be crucial in this model. Indeed, we did observe alterations in mice with VBP treated MC38 tumors compared to the vehicle treated group. Cell counts of CD4⁺ and CD8⁺ T cell subsets, as well as CD4 and CD8 double negative T cells were decreased in tumors of VBP treated mice. When we analyzed the percentage of CD8⁺ T cells compared to all T cells however, we detected a significant increase of CD8⁺ T cells in VBP treated tumors (Fig.4B,C). Furthermore, IFN γ ⁺CD44⁺ expressing T cells were significantly upregulated in percentage to all CD8⁺ T cells in VBP treated MC38 tumors (Fig.4D,E). These results indicate a possible effector function of CD8 T cells, that may be IFN γ mediated.

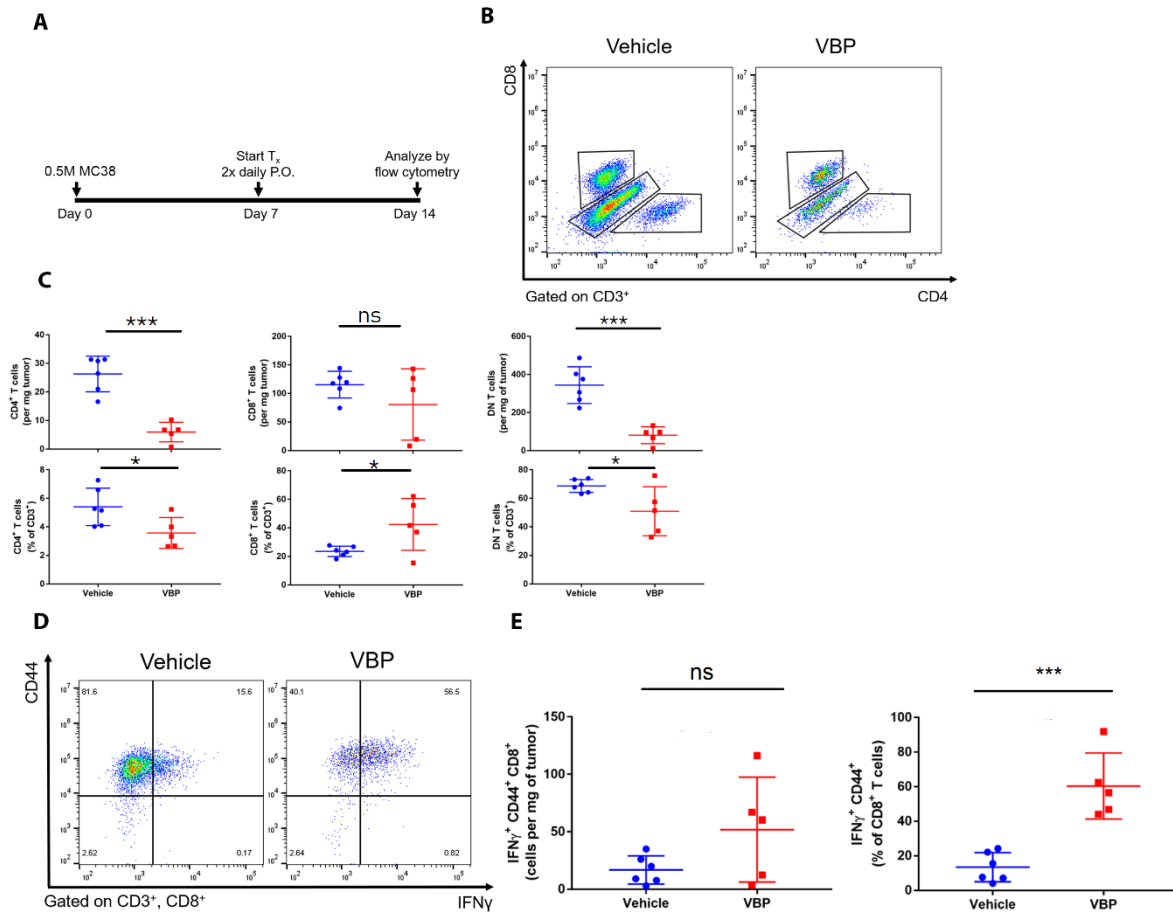


Fig. 4: T cell produce IFN γ in response to VBP

A Experimental Outlay of Flow Cytometry experiments seen in B-E. 0.5 Million MC38 cells were injected into C57/BL6 mice. Treatment (T_x) with VBP (20 μ g) or vehicle 2x/day p.o. was started on day 7 after injection and continued for a week. Mice were sacrificed on day 14 and tissue was analyzed through flow cytometry. **B** Representative flow cytometry data of CD3⁺CD4⁺, CD3⁺CD8⁺ and CD3⁺CD4⁺CD8⁺ T cell subset detected in MC38 tumors from WT C57BL/6 mice treated with VBP (n=4) or vehicle (n=6). **C** Quantification of T cell subsets seen in B in cell counts per mg of tumor and in percentage of all CD3⁺ T cells. Significance was calculated using an unpaired t-test, p=0.2370 (ns), p=0.329 (*), p=0.0001 (***). **D** Representative flow cytometry data for CD44⁺IFN γ ⁺ producing CD8⁺ T cells detected in MC38 tumors from mice treated with VBP (n=5) or vehicle (n=6). **E** Quantification of CD44⁺IFN γ ⁺ as seen in D in cell counts per mg of tumor or in percentage of all CD8⁺ T cells. Significance was calculated using an unpaired t-test, p=1018 (ns), p=0.0004.

We hypothesize that an interaction of Neutrophils and T cells is crucial for VBP mediated tumor growth suppression. To test this hypothesis, we attempted to deplete neutrophils in the Yummer1.7 tumor model using anti-Ly6G depleting antibody. Mice were treated with VBP and given either α Ly6G antibody in order to deplete neutrophils or an isotype control for 21 days, starting 3 days prior to Yummer1.7 cell injection. No differences in tumor growth were observed between the mice treated with anti-Ly6G antibody and the isotype control group (Fig.5A). When we validated neutrophil depletion in these mice on day 19 by flow cytometry, defining neutrophils as CD45⁺SSC^{high}.Ly6C^{interm.}, we did not detect a significant decrease in neutrophils in the anti-Ly6G treated group (Fig.5B,C). Here we use CD45⁺SSC^{high}Ly6C^{interm.} to define neutrophils instead of the otherwise used CD11b⁺Ly6G⁺ strategy, as the Ly6G receptor is presumably blocked by the anti-Ly6G antibody. We therefore found neutrophil

depletion using α Ly6G antibody to be ineffective in C57/BL6 mice. As suggested by a previous study (Faget et al. 2018) we then used anti-Ly6G antibody in combination with a secondary anti-rat antibody. The reason for this approach is that the anti-Ly6G antibody, which has proven to be ineffective for neutrophil depletion, is a ratIgG2a isotype orthologous to the mouse IgG1 heavy chain. The anti-Gr1 antibody, which targets Ly6G and Ly6c and effectively depletes neutrophils and monocytes, on the other hand is a ratIgG2b isotype orthologous to the mouse IgG2a heavy chain²². This difference in isotype might be the reason why the anti-Ly6G antibody mediated depletion is ineffective. The combination of the anti-Ly6G antibody with a mouse IgG2a antibody recognizing the rat IgGk light chain was shown to achieve neutrophil depletion in mice (Faget et al. 2018). Unfortunately, we did not observe neutrophil depletion in a 2 week long MC38 growth curve experiment with WT C57/BL6, using this method (Fig.5D,E). We therefore, do not recommend this approach for neutrophil depletion for experiments exceeding 9 days.

Taken together, our results highlight the importance of the Nlrp1 inflammasome in VBP induced tumor immunity in C57/BL6 mice and we further identified IL-18 as a crucial molecule, mediating this process. Investigating the cellular response, we observed an increase in IFN γ producing CD8⁺ T cells in MC38 tumors treated with VBP, which might act as tumor killing effector cells. We hypothesize that neutrophils might interact with T cells and contribute to tumor immunity. Due to lack of suitable neutrophil depletion methods, we were unable to investigate this theory any further *in vivo*, but other approaches can be applied, that will hopefully shed light to this question.

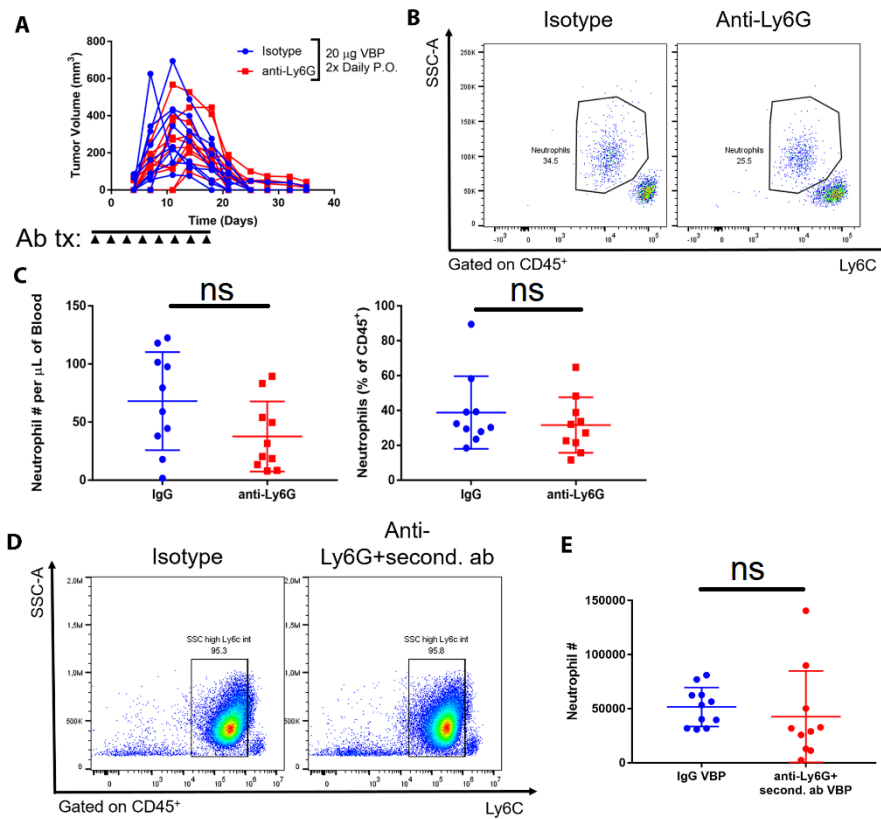


Fig. 5: Antibody based neutrophil depletion ineffective in our model

A Yumner1.7 tumor growth curves of mice administered anti-Ly6G antibody ($n=10$) or IgG Isotype control ($n=10$) treated with VBP. Antibody treatment was started 3 days before injection of 5 million Yumner1.7 cells and continued as indicated by the arrows. **B** Representative flow cytometry data of SSC-A^{high}Ly6C^{interm.} cells from blood of WT C57/BL6 mice injected with Yumner1.7 tumors treated with VBP and given anti-Ly6G antibody or IgG Isotype control. **C** Quantification of SSC-A^{high}Ly6C^{interm.} as seen in B in total cell counts and percentage of CD45⁺ cells mice injected with Yumner1.7 tumors treated with VBP and given anti-Ly6G antibody ($n=10$) or IgG Isotype control ($n=10$). Significance was calculated using an unpaired t-test, $p=0.3975$. **D** Representative flow cytometry data of SSC-A^{high}Ly6C^{interm.} cells from blood of WT C57/BL6 mice injected with MC38 tumors treated with VBP and given anti-Ly6G antibody in combination with a secondary anti-rat antibody or IgG Isotype control. **E** Quantification of SSC-A^{high}Ly6C^{interm.} as seen in D in total cell counts from cells from blood of WT C57/BL6 mice injected with MC38 tumors treated with VBP and given anti-Ly6G antibody in combination with a secondary anti-rat antibody ($n=10$) or IgG Isotype control ($n=11$). Significance was calculated using an unpaired t-test, $p=0.5275$ (ns).

6 Discussion

Cancer immunotherapy truly revolutionized cancer therapy and was named “breakthrough of the year” by *Science* in 2013. Immunotherapeutic treatment has been used in the clinic for years and has already benefited a lot of cancer patients. Nonetheless, not all cancer patients respond and adverse effects caused by the treatment are still a major concern. Further research is necessary to improve currently used immunotherapies, to not only make them more effective in a broader mass of cancer patients, but also to improve safety of the treatment. As most of the currently used cancer immunotherapies, like checkpoint inhibition, target the adaptive immune system to enhance anti-tumor immunity, we believe developing alternative strategies will lead to therapeutic improvement. Targeting the innate immune system for example, could be critical to achieve better responses in patients. Those therapies might be used as an adjuvants in combination with checkpoint inhibitors to increase anti-tumor immunity or might even induce a sufficient immune response alone.

In this study we showed that activating the Nlrp1 inflammasome through the amino-boronic dipeptide VBP leads to significant tumor growth inhibition in mice. We further showed that this effect is Casp1 dependent and identified the pro-inflammatory cytokine IL-18 to be crucial in the VBP induced tumor growth suppressing response. Investigation of the cellular response revealed systemic neutrophilia in VBP treated animals and an increase in IFN γ producing CD8 T cells in MC38 tumors upon VBP treatment. From previous studies we know that the adaptive immune system is essential for VBP induced anti-tumor immunity (Adams et al. 2004; Walsh et al. 2013). The role of neutrophils in our model remains however, unclear. To test if neutrophils are functional here, we aim to deplete neutrophils *in vivo*. We demonstrated that antibody based depletion strategies are not suitable for effective neutrophil depletion in our experiments. We will therefore plan to use MRP8Cre-DTR or MRP8Cre-DTA mice (Reber et al. 2017), a genetic mouse model that has been validated to conditionally lack neutrophils (Faget et al. 2018). These mice will be used in tumor growth curve experiments to test the functionality of neutrophils in VBP induced anti-tumor immunity.

IFN γ producing CD8 T cells are very likely the effector cells that lead to tumor growth inhibition in our model. To test this, tumor growth curve experiments in Rag mice or in mice in which CD8 T cells are depleted through an anti-CD8 antibody, need to be performed. We are further interested in interactions of innate immune cells with T cells during killing of tumor cells. We hypothesize that cells of the innate immune system, like neutrophils, might be polarized towards a tumor growth inhibiting phenotype through VBP. Contributions of cell-cell interactions as well as released cytokines in tumor killing can be tested through *in-vitro* killing assays. Thereby, T cell mediated tumor cell killing will be monitored in the presence of candidate cytokines or in co-culture with innate immune cells, like neutrophils. Of course, direct killing of tumor cells through innate immune cells can be investigated through this strategy as well. In

addition live imaging of these setups can be performed to visualize cell interactions and effector functions leading to tumor killing. To further characterize and assess effector functions of tumor infiltrating immune cells, we propose single cell sequencing of MC38 and Yummer1.7 tumors treated with VBP or vehicle.

Our results indicate that the VBP induced anti-tumor immunity depends on Nlrp1 signaling and cytokine release through a lytic form of cell death called pyroptosis. We next have to address the question, which cell compartment the pyroptosing cells consist of. Myeloid cells are promising candidates (Okondo et al. 2017). In order to determine which cell subset pyroptoses in response to VBP, we will use mice with conditional Casp1 deletion in various candidate cell types. These mice can then be used in tumor growth curve experiments. To specifically test if myeloid cells are indeed the pyroptosing cell type, Casp1 floxed mice crossed to mice expressing Cre recombinase under a Lysm promoter will be utilized. To further characterize and detect the location of the pyroptosing cells, inflammasome activation can be investigated *in vivo* by monitoring the subcellular localization of Asc in tissue of ASC-Citrine. These mice express a fluorescent ASC adaptor fusion protein, which retains the endogenous function of ASC. Inflammasome activation will lead to fluorescent speck formation that can be analyzed through microscopy or flow cytometry.

These experiments will be crucial to better understand the cellular response to VBP and will unravel yet unknown biology regarding interactions of the innate and adaptive immune system in tumor killing. While revealing the working mechanism of VBP will lay path to a better understanding of the role of the inflammasome in cancer immunotherapy, we need to remember that VBP does not lead to Nlrp1 inflammasome activation or tumor growth suppression in humans. Hence, investigating the role of other inflammasome sensors that can be pharmacologically activated in humans, to achieve anti-tumor immunity will be of utmost interest. In preliminary experiments, we indeed observed tumor growth suppression in tamoxifen inducible Nlrp3^{A350V} gain of function mice, in which the Nlrp3 inflammasome is constitutively active. Nlrp3 is a particularly promising pharmacological target, as it can be activated through homeostatic alteration of the cell (Martinon et al. 2002). Another candidate inflammasome sensor is human CARD8, due to its similarity to mouse Nlrp1. Activators of these inflammasome sensors can be identified through pharmacological screens and then be tested *in vivo*.

Overall our studies confirmed that targeting the inflammasome to enhance anti-tumor immunity is a promising strategy for development of new immunotherapies. Utilizing inflammasome activation as an adjuvants in combination with checkpoint inhibition might lead to enhanced anti-tumor immunity. However, further studies need to be conducted, to elucidate the mechanism of how inflammasome activation leads to tumor growth inhibition, including the cytokines involved, the cellular interactions and effector functions that lead to tumor killing.

7 Table of Figures

Fig. 1: VBP induced anti-tumor immunity depends on the Nlrp1 inflammasome.....	16
Fig. 2: IL-18 mediates VBP induced tumor growth suppression.....	18
Fig. 3: VBP treatment leads to systemic neutrophilia.....	20
Fig. 4: T cell produce IFN γ in response to VBP.....	22
Fig. 5: Antibody based neutrophil depletion ineffective in our model.....	24

8 References

- Adams S, Miller GT, Jesson MI, Watanabe T, Jones B, Wallner BP (2004) PT-100, a small molecule dipeptidyl peptidase inhibitor, has potent antitumor effects and augments antibody-mediated cytotoxicity via a novel immune mechanism. *Cancer Res* 64 (15):5471-5480. doi:10.1158/0008-5472.CAN-04-0447
- Badieyan ZS, Hoseini SS (2018) Adverse Effects Associated with Clinical Applications of CAR Engineered T Cells. *Arch Immunol Ther Exp (Warsz)* 66 (4):283-288. doi:10.1007/s00005-018-0507-9
- Bohn E, Sing A, Zumbihl R, Bielfeldt C, Okamura H, Kurimoto M, Heesemann J, Autenrieth IB (1998) IL-18 (IFN-gamma-inducing factor) regulates early cytokine production in, and promotes resolution of, bacterial infection in mice. *J Immunol* 160 (1):299-307
- Boyden ED, Dietrich WF (2006) Nalp1b controls mouse macrophage susceptibility to anthrax lethal toxin. *Nat Genet* 38 (2):240-244. doi:10.1038/ng1724
- Broz P, Dixit VM (2016) Inflammasomes: mechanism of assembly, regulation and signalling. *Nat Rev Immunol* 16 (7):407-420. doi:10.1038/nri.2016.58
- Case CL, Kohler LJ, Lima JB, Strowig T, de Zoete MR, Flavell RA, Zamboni DS, Roy CR (2013) Caspase-11 stimulates rapid flagellin-independent pyroptosis in response to *Legionella pneumophila*. *Proc Natl Acad Sci U S A* 110 (5):1851-1856. doi:10.1073/pnas.1211521110
- Chamoto K, Al-Habsi M, Honjo T (2017) Role of PD-1 in Immunity and Diseases. *Curr Top Microbiol Immunol* 410:75-97. doi:10.1007/82_2017_67
- Chavarria-Smith J, Vance RE (2015) The NLRP1 inflammasomes. *Immunol Rev* 265 (1):22-34. doi:10.1111/imr.12283
- Chen GY, Nunez G (2011) Inflammasomes in intestinal inflammation and cancer. *Gastroenterology* 141 (6):1986-1999. doi:10.1053/j.gastro.2011.10.002
- Chow MT, Ozga AJ, Servis RL, Frederick DT, Lo JA, Fisher DE, Freeman GJ, Boland GM, Luster AD (2019) Intratumoral Activity of the CXCR3 Chemokine System Is Required for the Efficacy of Anti-PD-1 Therapy. *Immunity* 50 (6):1498-1512 e1495. doi:10.1016/j.immuni.2019.04.010
- Coffelt SB, Kersten K, Doornebal CW, Weiden J, Vrijland K, Hau CS, Verstegen NJM, Ciampricotti M, Hawinkels L, Jonkers J, de Visser KE (2015) IL-17-producing gammadelta T cells and neutrophils conspire to promote breast cancer metastasis. *Nature* 522 (7556):345-348. doi:10.1038/nature14282
- Colegio OR, Chu NQ, Szabo AL, Chu T, Rhebergen AM, Jairam V, Cyrus N, Brokowski CE, Eisenbarth SC, Phillips GM, Cline GW, Phillips AJ, Medzhitov R (2014) Functional polarization of tumour-associated macrophages by tumour-derived lactic acid. *Nature* 513 (7519):559-563. doi:10.1038/nature13490
- Colotta F, Allavena P, Sica A, Garlanda C, Mantovani A (2009) Cancer-related inflammation, the seventh hallmark of cancer: links to genetic instability. *Carcinogenesis* 30 (7):1073-1081. doi:10.1093/carcin/bgp127
- Couzin-Frankel J (2013) Breakthrough of the year 2013. Cancer immunotherapy. *Science* 342 (6165):1432-1433. doi:10.1126/science.342.6165.1432
- Di Virgilio F (2013) The therapeutic potential of modifying inflammasomes and NOD-like receptors. *Pharmacol Rev* 65 (3):872-905. doi:10.1124/pr.112.006171
- Dominguez C, McCampbell KK, David JM, Palena C (2017) Neutralization of IL-8 decreases tumor PMN-MDSCs and reduces mesenchymalization of claudin-low triple-negative breast cancer. *JCI Insight* 2 (21). doi:10.1172/jci.insight.94296
- Dupaul-Chicoine J, Arabzadeh A, Dagenais M, Douglas T, Champagne C, Morizot A, Rodrigue-Gervais IG, Breton V, Colpitts SL, Beauchemin N, Saleh M (2015) The Nlrp3 Inflammasome Suppresses Colorectal Cancer Metastatic Growth in the Liver by Promoting Natural Killer Cell Tumoricidal Activity. *Immunity* 43 (4):751-763. doi:10.1016/j.immuni.2015.08.013
- Esmailbeig M, Ghaderi A (2017) Interleukin-18: a regulator of cancer and autoimmune diseases. *Eur Cytokine Netw* 28 (4):127-140. doi:10.1684/ecn.2018.0401

- Faget J, Boivin G, Ancey P-B, Gkasti A, Mussard J, Engblom C, Pfirschke C, Vazquez J, Bendriss-Vermare N, Caux C, Vozenin M-C, Pittet MJ, Gunzer M, Meylan E (2018) Efficient and specific Ly6G⁺ cell depletion: A change in the current practices toward more relevant functional analyses of neutrophils. *bioRxiv*:498881. doi:10.1101/498881
- Finger JN, Lich JD, Dare LC, Cook MN, Brown KK, Duraiswami C, Bertin J, Gough PJ (2012) Autolytic proteolysis within the function to find domain (FIIND) is required for NLRP1 inflammasome activity. *J Biol Chem* 287 (30):25030-25037. doi:10.1074/jbc.M112.378323
- Franchi L, Munoz-Planillo R, Nunez G (2012) Sensing and reacting to microbes through the inflammasomes. *Nat Immunol* 13 (4):325-332. doi:10.1038/ni.2231
- Fridlender ZG, Sun J, Kim S, Kapoor V, Cheng G, Ling L, Worthen GS, Albelda SM (2009) Polarization of tumor-associated neutrophil phenotype by TGF-beta: "N1" versus "N2" TAN. *Cancer Cell* 16 (3):183-194. doi:10.1016/j.ccr.2009.06.017
- Gabrilovich DI (2017) Myeloid-Derived Suppressor Cells. *Cancer Immunol Res* 5 (1):3-8. doi:10.1158/2326-6066.CIR-16-0297
- Gai K, Okondo MC, Rao SD, Chui AJ, Ball DP, Johnson DC, Bachovchin DA (2019) DPP8/9 inhibitors are universal activators of functional NLRP1 alleles. *Cell Death Dis* 10 (8):587. doi:10.1038/s41419-019-1817-5
- Galon J, Bruni D (2019) Approaches to treat immune hot, altered and cold tumours with combination immunotherapies. *Nat Rev Drug Discov* 18 (3):197-218. doi:10.1038/s41573-018-0007-y
- Glaccum MB, Stocking KL, Charrier K, Smith JL, Willis CR, Maliszewski C, Livingston DJ, Peschon JJ, Morrissey PJ (1997) Phenotypic and functional characterization of mice that lack the type I receptor for IL-1. *J Immunol* 159 (7):3364-3371
- Gomes-Silva D, Ramos CA (2018) Cancer Immunotherapy Using CAR-T Cells: From the Research Bench to the Assembly Line. *Biotechnol J* 13 (2). doi:10.1002/biot.201700097
- Gonzalez H, Hagerling C, Werb Z (2018) Roles of the immune system in cancer: from tumor initiation to metastatic progression. *Genes Dev* 32 (19-20):1267-1284. doi:10.1101/gad.314617.118
- Hanahan D, Weinberg RA (2011) Hallmarks of cancer: the next generation. *Cell* 144 (5):646-674. doi:10.1016/j.cell.2011.02.013
- Karki R, Man SM, Kanneganti TD (2017) Inflammasomes and Cancer. *Cancer Immunol Res* 5 (2):94-99. doi:10.1158/2326-6066.CIR-16-0269
- Kolb R, Liu GH, Janowski AM, Sutterwala FS, Zhang W (2014) Inflammasomes in cancer: a double-edged sword. *Protein Cell* 5 (1):12-20. doi:10.1007/s13238-013-0001-4
- Kovarova M, Hesker PR, Jania L, Nguyen M, Snouwaert JN, Xiang Z, Lommatzsch SE, Huang MT, Ting JP, Koller BH (2012) NLRP1-dependent pyroptosis leads to acute lung injury and morbidity in mice. *J Immunol* 189 (4):2006-2016. doi:10.4049/jimmunol.1201065
- Li Y, Wang L, Pappan L, Galliher-Beckley A, Shi J (2012) IL-1beta promotes stemness and invasiveness of colon cancer cells through Zeb1 activation. *Mol Cancer* 11:87. doi:10.1186/1476-4598-11-87
- Malik A, Kanneganti TD (2017) Inflammasome activation and assembly at a glance. *J Cell Sci* 130 (23):3955-3963. doi:10.1242/jcs.207365
- Marcus A, Gowen BG, Thompson TW, Iannello A, Ardolino M, Deng W, Wang L, Shifrin N, Raulet DH (2014) Recognition of tumors by the innate immune system and natural killer cells. *Adv Immunol* 122:91-128. doi:10.1016/B978-0-12-800267-4.00003-1
- Martinon F, Burns K, Tschopp J (2002) The inflammasome: a molecular platform triggering activation of inflammatory caspases and processing of proIL-beta. *Mol Cell* 10 (2):417-426. doi:10.1016/s1097-2765(02)00599-3
- Masters SL, Gerlic M, Metcalf D, Preston S, Pellegrini M, O'Donnell JA, McArthur K, Baldwin TM, Chevrier S, Nowell CJ, Cengia LH, Henley KJ, Collinge JE, Kastner DL, Feigenbaum L, Hilton DJ, Alexander WS, Kile BT, Croker BA (2012) NLRP1 inflammasome activation induces pyroptosis of hematopoietic progenitor cells. *Immunity* 37 (6):1009-1023. doi:10.1016/j.immuni.2012.08.027

- Negrini S, Gorgoulis VG, Halazonetis TD (2010) Genomic instability--an evolving hallmark of cancer. *Nat Rev Mol Cell Biol* 11 (3):220-228. doi:10.1038/nrm2858
- Ohri CM, Shikotra A, Green RH, Waller DA, Bradding P (2009) Macrophages within NSCLC tumour islets are predominantly of a cytotoxic M1 phenotype associated with extended survival. *Eur Respir J* 33 (1):118-126. doi:10.1183/09031936.00065708
- Okondo MC, Johnson DC, Sridharan R, Go EB, Chui AJ, Wang MS, Poplawski SE, Wu W, Liu Y, Lai JH, Sanford DG, Arciprete MO, Golub TR, Bachovchin WW, Bachovchin DA (2017) DPP8 and DPP9 inhibition induces pro-caspase-1-dependent monocyte and macrophage pyroptosis. *Nat Chem Biol* 13 (1):46-53. doi:10.1038/nchembio.2229
- Pardoll DM (2012) The blockade of immune checkpoints in cancer immunotherapy. *Nat Rev Cancer* 12 (4):252-264. doi:10.1038/nrc3239
- Ponzetta A, Carriero R, Carnevale S, Barbagallo M, Molgora M, Perucchini C, Magrini E, Gianni F, Kunderfranco P, Polentarutti N, Pasqualini F, Di Marco S, Supino D, Peano C, Cananzi F, Colombo P, Pilotti S, Alomar SY, Bonavita E, Galdiero MR, Garlanda C, Mantovani A, Jaillon S (2019) Neutrophils Driving Unconventional T Cells Mediate Resistance against Murine Sarcomas and Selected Human Tumors. *Cell* 178 (2):346-360 e324. doi:10.1016/j.cell.2019.05.047
- Qian BZ, Pollard JW (2010) Macrophage diversity enhances tumor progression and metastasis. *Cell* 141 (1):39-51. doi:10.1016/j.cell.2010.03.014
- Reber LL, Gillis CM, Starkl P, Jonsson F, Sibilano R, Marichal T, Gaudenzio N, Berard M, Rogalla S, Contag CH, Bruhns P, Galli SJ (2017) Neutrophil myeloperoxidase diminishes the toxic effects and mortality induced by lipopolysaccharide. *J Exp Med* 214 (5):1249-1258. doi:10.1084/jem.20161238
- Ribas A, Wolchok JD (2018) Cancer immunotherapy using checkpoint blockade. *Science* 359 (6382):1350-1355. doi:10.1126/science.aar4060
- Ridker PM, MacFadyen JG, Thuren T, Everett BM, Libby P, Glynn RJ, Group CT (2017) Effect of interleukin-1beta inhibition with canakinumab on incident lung cancer in patients with atherosclerosis: exploratory results from a randomised, double-blind, placebo-controlled trial. *Lancet* 390 (10105):1833-1842. doi:10.1016/S0140-6736(17)32247-X
- Salcedo R, Worschech A, Cardone M, Jones Y, Gyulai Z, Dai RM, Wang E, Ma W, Haines D, O'HUigin C, Marincola FM, Trinchieri G (2010) MyD88-mediated signaling prevents development of adenocarcinomas of the colon: role of interleukin 18. *J Exp Med* 207 (8):1625-1636. doi:10.1084/jem.20100199
- Savoia P, Astrua C, Fava P (2016) Ipilimumab (Anti-Ctla-4 Mab) in the treatment of metastatic melanoma: Effectiveness and toxicity management. *Hum Vaccin Immunother* 12 (5):1092-1101. doi:10.1080/21645515.2015.1129478
- Schietinger A, Philip M, Schreiber H (2008) Specificity in cancer immunotherapy. *Semin Immunol* 20 (5):276-285. doi:10.1016/j.smim.2008.07.001
- Schroder K, Tschopp J (2010) The inflammasomes. *Cell* 140 (6):821-832. doi:10.1016/j.cell.2010.01.040
- Shaul ME, Fridlender ZG (2017) Neutrophils as active regulators of the immune system in the tumor microenvironment. *J Leukoc Biol* 102 (2):343-349. doi:10.1189/jlb.5MR1216-508R
- Shi J, Zhao Y, Wang K, Shi X, Wang Y, Huang H, Zhuang Y, Cai T, Wang F, Shao F (2015) Cleavage of GSDMD by inflammatory caspases determines pyroptotic cell death. *Nature* 526 (7575):660-665. doi:10.1038/nature15514
- Steer HJ, Lake RA, Nowak AK, Robinson BW (2010) Harnessing the immune response to treat cancer. *Oncogene* 29 (48):6301-6313. doi:10.1038/onc.2010.437
- Takeda K, Tsutsui H, Yoshimoto T, Adachi O, Yoshida N, Kishimoto T, Okamura H, Nakanishi K, Akira S (1998) Defective NK cell activity and Th1 response in IL-18-deficient mice. *Immunity* 8 (3):383-390. doi:10.1016/s1074-7613(00)80543-9
- Tu S, Bhagat G, Cui G, Takaishi S, Kurt-Jones EA, Rickman B, Betz KS, Penz-Oesterreicher M, Bjorkdahl O, Fox JG, Wang TC (2008) Overexpression of interleukin-1beta induces gastric inflammation

- and cancer and mobilizes myeloid-derived suppressor cells in mice. *Cancer Cell* 14 (5):408-419. doi:10.1016/j.ccr.2008.10.011
- Tumeh PC, Harview CL, Yearley JH, Shintaku IP, Taylor EJ, Robert L, Chmielowski B, Spasic M, Henry G, Ciobanu V, West AN, Carmona M, Kivork C, Seja E, Cherry G, Gutierrez AJ, Grogan TR, Mateus C, Tomasic G, Glaspy JA, Emerson RO, Robins H, Pierce RH, Elashoff DA, Robert C, Ribas A (2014) PD-1 blockade induces responses by inhibiting adaptive immune resistance. *Nature* 515 (7528):568-571. doi:10.1038/nature13954
- Walsh MP, Duncan B, Larabee S, Krauss A, Davis JP, Cui Y, Kim SY, Guimond M, Bachovchin W, Fry TJ (2013) Val-boroPro accelerates T cell priming via modulation of dendritic cell trafficking resulting in complete regression of established murine tumors. *PLoS One* 8 (3):e58860. doi:10.1371/journal.pone.0058860
- Wang J, Perry CJ, Meeth K, Thakral D, Damsky W, Micevic G, Kaech S, Blenman K, Bosenberg M (2017) UV-induced somatic mutations elicit a functional T cell response in the YUMMER1.7 mouse melanoma model. *Pigment Cell Melanoma Res* 30 (4):428-435. doi:10.1111/pcmr.12591
- Wolchok JD, Chiarion-Sileni V, Gonzalez R, Rutkowski P, Grob JJ, Cowey CL, Lao CD, Wagstaff J, Schadendorf D, Ferrucci PF, Smylie M, Dummer R, Hill A, Hogg D, Haanen J, Carlino MS, Bechter O, Maio M, Marquez-Rodas I, Guidoboni M, McArthur G, Lebbe C, Ascierto PA, Long GV, Cebon J, Sosman J, Postow MA, Callahan MK, Walker D, Rollin L, Bhore R, Hodi FS, Larkin J (2017) Overall Survival with Combined Nivolumab and Ipilimumab in Advanced Melanoma. *N Engl J Med* 377 (14):1345-1356. doi:10.1056/NEJMoa1709684
- Woo SR, Fuertes MB, Corrales L, Spranger S, Furdyna MJ, Leung MY, Duggan R, Wang Y, Barber GN, Fitzgerald KA, Alegre ML, Gajewski TF (2014) STING-dependent cytosolic DNA sensing mediates innate immune recognition of immunogenic tumors. *Immunity* 41 (5):830-842. doi:10.1016/j.immuni.2014.10.017
- Yao Y, Chen S, Cao M, Fan X, Yang T, Huang Y, Song X, Li Y, Ye L, Shen N, Shi Y, Li X, Wang F, Qian Y (2017) Antigen-specific CD8(+) T cell feedback activates NLRP3 inflammasome in antigen-presenting cells through perforin. *Nat Commun* 8:15402. doi:10.1038/ncomms15402
- Zaki MH, Vogel P, Body-Malapel M, Lamkanfi M, Kanneganti TD (2010) IL-18 production downstream of the Nlrp3 inflammasome confers protection against colorectal tumor formation. *J Immunol* 185 (8):4912-4920. doi:10.4049/jimmunol.1002046
- Zaretsky JM, Garcia-Diaz A, Shin DS, Escuin-Ordinas H, Hugo W, Hu-Lieskovan S, Torrejon DY, Abril-Rodriguez G, Sandoval S, Barthly L, Saco J, Homet Moreno B, Mezzadra R, Chmielowski B, Ruchalski K, Shintaku IP, Sanchez PJ, Puig-Saus C, Cherry G, Seja E, Kong X, Pang J, Berent-Maoz B, Comin-Anduix B, Graeber TG, Tumeh PC, Schumacher TN, Lo RS, Ribas A (2016) Mutations Associated with Acquired Resistance to PD-1 Blockade in Melanoma. *N Engl J Med* 375 (9):819-829. doi:10.1056/NEJMoa1604958
- Zhang M, He Y, Sun X, Li Q, Wang W, Zhao A, Di W (2014) A high M1/M2 ratio of tumor-associated macrophages is associated with extended survival in ovarian cancer patients. *J Ovarian Res* 7:19. doi:10.1186/1757-2215-7-19
- Zhong FL, Mamai O, Sborgi L, Boussofara L, Hopkins R, Robinson K, Szeverenyi I, Takeichi T, Balaji R, Lau A, Tye H, Roy K, Bonnard C, Ahl PJ, Jones LA, Baker PJ, Lacina L, Otsuka A, Fournie PR, Malecaze F, Lane EB, Akiyama M, Kabashima K, Connolly JE, Masters SL, Soler VJ, Omar SS, McGrath JA, Nedelcu R, Gribaa M, Denguezli M, Saad A, Hiller S, Reversade B (2016) Germline NLRP1 Mutations Cause Skin Inflammatory and Cancer Susceptibility Syndromes via Inflammasome Activation. *Cell* 167 (1):187-202 e117. doi:10.1016/j.cell.2016.09.001